J. Fluid Mech. (1984), *vol.* 147, *pp.* 315–332
Printed in Great Britain

Unsteady boundary layers close to the stagnation region of slender bodies

By TUNCER CEBECI,
Aerodynamics Research & Technology,
Douglas Aircraft Company, Long Beach, CA

KEITH STEWARTSON†
Department of Mathematics,
University College, London

AND SUZANNE M. SCHIMKE
Aerodynamics Research & Technology, Douglas Aircraft Company, Long Beach, CA

(Received 13 October 1983 and in revised form 21 May 1984)

The evolution of unsteady boundary layers on the plane of symmetry of a slender prolate spheroid in uniform motion at constant angle of attack after an impulsive start has been studied for the case of a prescribed pressure distribution. Calculated results have been obtained for angles of attack ranging from 30° to 50° and show, for example, that the unsteady-state solutions approach the steady-state solutions rapidly on the windward and leeward sides for $\alpha < \alpha_c$ ($\approx 41°$). This is also so on the windward side for $\alpha > \alpha_c$. On the leeward side for $\alpha > \alpha_c$, however, the unsteady boundary layer is initially unseparated, but develops a region of reversed flow with increasing time. Subsequently, the streamwise displacement thickness develops a pronounced peak, which leads to a singularity of the type observed by van Dommelen & Shen on a circular cylinder started impulsively from rest.

1. Introduction

Our knowledge of unsteady boundary layers has been enhanced in recent years by a combination of experimental and computational investigations. The former have been concerned mainly with the problem of airfoils that oscillate in subsonic flows, but include a small number of transonic-flow investigations. The latter have involved the solution of boundary-layer equations for flows over cylinders and airfoils, and have been concerned largely with the nature of the singularity which occurs near separation. Solutions of the Navier–Stokes equations have also been obtained to provide an overall understanding of the flow patterns at conditions near or at dynamic stall. Useful reviews of previous work have been provided by Telionis (1979), McCroskey (1982), Williams (1977) and Cebeci (1982).

The experimental investigations have been carried out mainly to improve understanding of flow around helicopter rotor blades, and include the low-speed measurements of McCroskey *et al.* (1982), Carr, McAlister & McCroskey (1977), Carr & McAlister (1983), Young (1982), Geissler (1983) and Cousteix, Houdeville & Janelle (1981), and transonic-flow measurements of Tijdeman (1977) and Davis & Malcolm (1979). The range of measurements of McCroskey *et al.* and Carr *et al.*, in particular, is extensive, and includes more than fifty combinations of Mach number and parameters of the unsteady motion for each of eight airfoil sections. As a consequence, four flow regimes have been identified, and correspond to no stall, stall onset, light stall and deep stall. It appears that the breakdown of the unsteady boundary layer

† Deceased 7 May 1983.

leads to a large vortex which is formed near the surface at large angles of attack and causes stall to occur shortly thereafter.

Computational investigations of oscillating-airfoil flows have been of two main types. In the first, solutions of the Navier–Stokes equations have been obtained, for example by Mehta (1977) for incompressible laminar flows and by Shamroth (1981) for compressible turbulent flows. Further studies of this type are clearly necessary, and results so far show qualitative features of the flow field and lift curves which are again in qualitative agreement with experiment. The second approach has involved the solution of the boundary-layer equations. The investigations of Cebeci & Carr (1981, 1983) have reported results for an external velocity distribution typical of those found near the leading edge of thin airfoils. The existence of a singularity in the solutions is evident in the vicinity of the leading edge at the higher angles of attack and has led to the subsequent investigations of its nature (see e.g. Cebeci, Khattab & Schimke 1983).

The need for more fundamental investigations of the use of boundary-layer equations to represent unsteady flows is clear from the airfoil investigations of the previous paragraph. In this connection, the oscillating-flat-plate investigations of Cousteix *et al.* (1981) and the contributions of Telionis & Tsahalis (1974), van Dommelen & Shen (1982*a*, *b*), Smith (1982) and Cebeci (1979, 1982) for flow over a cylinder impulsively started from rest are particularly relevant. In addition, Williams (1982) and Williams & Stewartson (1983) have made important contributions to our understanding of the nature of the singularity and its consequences. Perhaps the most important contribution has been that of van Dommelen & Shen (1982*a*), who solved the boundary-layer equations in Lagrangian form and revealed the existence of the singularity. This result suggests the need for interaction between the viscous- and inviscid-flow equations.

Though a number of studies have been conducted to improve our understanding of unsteady two-dimensional boundary layers, very little work has been done for unsteady three-dimensional flows. Experimental information is lacking, but the similarity between the two- and three-dimensional equations suggests that the same phenomena may occur. The three-dimensional boundary layer on a body of revolution at angle of attack is obviously more complicated than for airfoils or cylinders, but is similar on the line of symmetry, provided that cross-flow gradients are taken into account. In the case of steady flow past slender spheroids, it is known (see e.g. Cebeci, Khattab & Stewartson 1980) that separation does not occur on the leeward side until well past the maximum thickness if the angle of attack α is less than a critical value α_c ($\approx 41°$), but for $\alpha > \alpha_c$ there is a dramatic change, with separation occurring very close to the nose. If the external velocity is prescribed, this abruptly terminates the integration. For thin airfoils there is a parallel situation, as shown by Cebeci, Stewartson & Williams (1981*a*), but the critical angle is now of the order of magnitude of the airfoil thickness.

In this paper we report a study of the unsteady boundary layer on the line of symmetry to determine the relation between unsteady separation and singularities in the solution. For the first step we concentrate on the separation problem and do not consider the effect of moving stagnation points, which is important but adds considerably to the computational difficulties. The particular problem we study is the development of a boundary layer on a thin spheroid in uniform motion at constant angle of attack after an impulsive start. Angles of attack ranging from 30° to 50° are chosen for this purpose. Of these $\alpha = 45°$ corresponds to nose separation, which is marginal, while $\alpha = 50°$ corresponds to a strong steady-state singularity. The

problem has been formulated for the general case of spheroids at angles of attack and specialized to thin bodies, and specifically those for which the thickness ratio τ is vanishingly small.

2. Approach

With respect to a cylindrical-polar set of coordinates (x, r, θ) and origin O, let the equation of the spheroid be

$$\tau^2 x^2 + r^2 = \tau^2, \tag{1}$$

where τ is a positive number less than unity, which may be regarded as a measure of the thickness ratio of the prolate spheroid. Here we have non-dimensionalized the coordinates and time t, taking the semi-major axis and the velocity at infinity to be unity. We assume that at an infinite distance from the spheroid the velocity of the fluid is in a direction lying in the meridional plane at an angle α to its major axis. Further we assume that outside the boundary layer the inviscid flow is irrotational and attached and neglect the circulation around the spheroid. The achievement of our goal of determining the development of the boundary layer, given the mainstream velocity, would be an important step forward in the task of predicting the circulation around bodies of revolution at incidence.

With these assumptions the velocity of slip on the spheroid, according to inviscid theory, has components

$$\left.\begin{aligned} u_e &= V_0(\tau)\cos\alpha\cos\beta - V_{90}(\tau)\sin\alpha\sin\beta\cos\theta, \\ w_e &= V_{90}(\tau)\sin\alpha\sin\theta, \end{aligned}\right\} \tag{2}$$

where

$$V_0(\tau) = \frac{(1-\tau^2)^{\frac{3}{2}}}{(1-\tau^2)^{\frac{1}{2}} - \frac{1}{2}\tau^2 \log\dfrac{1+(1-\tau^2)^{\frac{1}{2}}}{1-(1-\tau^2)^{\frac{1}{2}}}}, \tag{3}$$

$$V_{90}(\tau) = \frac{2V_0(\tau)}{2V_0(\tau)-1},$$

$$\cos\beta = \frac{(1-x^2)^{\frac{1}{2}}}{[1+x^2(\tau^2-1)]^{\frac{1}{2}}}, \tag{4}$$

and α is a specified function of time, being constant in the present study. The configuration in the meridional plane is illustrated in figure 1, with S the stagnation point of the inviscid flow defined by $\theta = 0$, $x = -\{1-\tau^2\tan^2\alpha\}$.

Turning to the boundary layer, we define $(u, v\nu^{\frac{1}{2}}, w)$ to be the velocity components respectively along the meridional lines $\theta = \text{const}$, along the normals to the spheroid and in the azimuthal direction, where ν is the kinematic viscosity of the fluid and is assumed small. Then

$$\frac{\partial}{\partial x}(h_2 u) + \frac{\partial}{\partial\theta}(h_1 w) + \frac{\partial}{\partial y}(h_1 h_2 v) = 0, \tag{5}$$

$$\frac{\partial u}{\partial t} + \frac{u}{h_1}\frac{\partial u}{\partial x} + \frac{w}{h_2}\frac{\partial u}{\partial\theta} + v\frac{\partial u}{\partial y} + w^2 K_2 = -\frac{1}{h_1}\frac{\partial\hat{p}}{\partial x} + \frac{\partial^2 u}{\partial y^2}, \tag{6}$$

$$\frac{\partial u}{\partial t} + \frac{u}{h_1}\frac{\partial w}{\partial x} + \frac{w}{h_2}\frac{\partial w}{\partial\theta} + v\frac{\partial w}{\partial y} - uwK_2 = -\frac{1}{h_2}\frac{\partial\hat{p}}{\partial\theta} + \frac{\partial^2 w}{\partial y^2}, \tag{7}$$

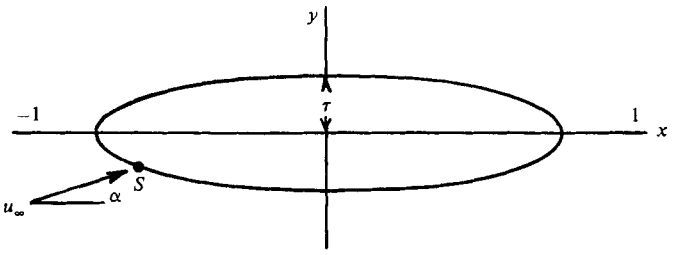

FIGURE 1. Notation for prolate spheroid.

where $y\nu^{\frac{1}{2}}$ measures distance along the outward-drawn normal from the body,

$$h_1 = \left[\frac{1+x^2(\tau^2-1)}{1-x^2}\right]^{\frac{1}{2}}, \quad h_2 = \tau(1-x^2)^{\frac{1}{2}} \tag{8}$$

are the metric coefficients,

$$K_2 = \frac{x}{[1+x^2(\tau^2-1)]^{\frac{1}{2}}(1-x^2)^{\frac{1}{2}}} \tag{9}$$

is the geodesic curvature of the surface lines $x = \text{const}$, and $\hat{p}$ is the reduced pressure. The appropriate boundary conditions are

$$\left.\begin{aligned} u = v = w = 0 \quad &\text{at} \quad y = 0, \\ u \to u_e, \quad w \to w_e \quad &\text{as} \quad y \to \infty. \end{aligned}\right\} \tag{10a}$$

The specification of the problem is completed by assigning initial conditions on u, w with respect to space and time. The spatial conditions are that on the line of symmetry $w = 0$ and u vanishes for all y at that value of x for which $u_e = 0$. This is physically and mathematically sensible for impulsive problems in which the stagnation point is fixed, but is not necessarily correct when the angle of attack is varying with time; see Cebeci & Carr (1981) for example. The temporal conditions are that at $t = 0$ both u and w vanish on the body $y = 0$ on the line of symmetry, but are equal to their external values elsewhere. Thus

$$\left.\begin{aligned} &u = w = 0 \quad \text{at} \quad y = 0, \quad t = 0 \quad \text{for all } x, \\ \text{while} \quad &u = u_e, \quad w = w_e \quad \text{for} \quad y > 0, \quad t = 0 \quad \text{and all } x. \end{aligned}\right\} \tag{10b}$$

In the early studies of the properties of the boundary layers on prolate spheroids conducted by Wang (1970) and Hirsh & Cebeci (1977), some difficulty was experienced in continuing the solution past the nose at $x = -1$, primarily because of the singularities in the properties of h_1, h_2 and K_2 there. A common procedure was first to perform the integration along the line of symmetry from the stagnation point to as near the nose as possible, and then to jump across the nose to the same value of x on the leeside ($\theta = \pi$) assuming that the flow properties are essentially unchanged. After that, integration on the leeside may be continued as far as separation. Afterwards the procedure may be extended to more general points in the neighbourhood of the nose. This technique is effective at moderate values of τ ($\tau = 1$ corresponds to a sphere), but leads to difficulties as $\tau \to 0$, especially at high angles of attack. Cebeci *et al.* (1980) demonstrated that the singularity may be removed by a suitable transformation of the surface coordinate system, enabling a smooth passage to be made around the nose. The transformation is equally effective for unsteady boundary layers, and is now explained for the limiting case of a paraboloid which corresponds to $\tau = 0$.

The first step is to define new surface coordinates by

$$\left.\begin{aligned} \frac{\mathrm{d}S}{S} &= \frac{h_1\,\mathrm{d}x}{h_2} = \frac{[1+x^2(\tau^2-1)]^{\frac{1}{2}}}{\tau(1-x^2)}\mathrm{d}x, \\ X = S\cos\theta, \quad Z &= S\sin\theta, \quad Y = \frac{y}{\tau}, \quad T = \frac{t}{\tau^2} \end{aligned}\right\} \tag{11}$$

with $S = 0$ at $x = -1$, and new velocity components by

$$u = U\cos\theta + W\sin\theta, \quad w = W\cos\theta - U\sin\theta, \quad v = \frac{V}{\tau}. \tag{12}$$

The purpose of this transformation is to convert the polar form of (5)–(7) into a quasi-rectangular-Cartesian form which is free of singularities. The governing equations reduce to

$$N\left(\frac{\partial U}{\partial X}+\frac{\partial W}{\partial Z}\right)+\frac{\partial V}{\partial Y}-L(UX+WZ) = 0, \tag{13}$$

$$\frac{\partial U}{\partial T}+N\left(U\frac{\partial U}{\partial X}+W\frac{\partial U}{\partial Z}\right)+LW(WX-UZ)+V\frac{\partial U}{\partial Y} = \tilde{\beta}_1+\frac{\partial^2 U}{\partial Y^2}, \tag{14}$$

$$\frac{\partial W}{\partial T}+N\left(U\frac{\partial W}{\partial X}+W\frac{\partial W}{\partial Z}\right)-LU(WX-UZ)+V\frac{\partial W}{\partial Y} = \tilde{\beta}_2+\frac{\partial^2 W}{\partial Y^2}, \tag{15}$$

where $\tilde{\beta}_1, \tilde{\beta}_2$ are pressure-gradient parameters defined by the requirement that $u \to u_e$, $w \to w_e$ as $Y \to \infty$ and

$$N = \frac{S\tau^2}{h_2}, \quad L = \frac{\tau^2}{S}\left(\frac{1}{h_2}+K_2\right). \tag{16}$$

For the paraboloid we let $\tau \to 0$ after defining

$$p = \frac{(1-x^2)^{\frac{1}{2}}}{\tau}, \tag{17}$$

when

$$S = \frac{p}{(1+p^2)^{\frac{1}{2}}+1}\exp\left[(1+p^2)^{\frac{1}{2}}-1\right], \tag{18}$$

$$N = \frac{S}{p}, \quad L = \frac{(1+p^2)^{\frac{1}{2}}-1}{pS(1+p^2)^{\frac{1}{2}}}, \tag{19}$$

and so (13)–(15) are independent of τ. We write (U_e, W_e) for the limits of $(u_e\cos\theta - w_e\sin\theta,\ u_e\sin\theta + w_e\cos\theta)$ as $\tau \to 0$, and then

$$U_e = \frac{pX\cos\alpha}{S(1+p^2)^{\frac{1}{2}}}-2\left(1-\frac{pX^2L}{S}\right)\sin\alpha, \tag{20}$$

$$W_e = \frac{pZ\cos\alpha}{S(1+p^2)^{\frac{1}{2}}}+\frac{2XZLp}{S}\sin\alpha, \tag{21}$$

so that

$$\tilde{\beta}_1 = N\left(U_e\frac{\partial U_e}{\partial X}+W_e\frac{\partial U_e}{\partial Z}\right)+LW_e(W_eX-U_eZ), \tag{22}$$

$$\tilde{\beta}_2 = N\left(U_e\frac{\partial W_e}{\partial X}+W_e\frac{\partial W_e}{\partial Z}\right)-LU_e(W_eX-U_eZ). \tag{23}$$

These equations are free of all geometric singularities, and in particular at the nose $p = 0$. There is therefore now no special problem about integrating the equations through the nose, although it should be noted that the equations are only appropriate

at distances from it corresponding to $p = O(1)$. This is the natural lengthscale for the paraboloid, but in terms of general thin axisymmetric bodies this distance is $O(\tau^2)$ from the nose.

Line-of-symmetry equations

These may be deduced from the general form (13) *et seq.* given above using similar arguments to those in Cebeci *et al.* (1981*b*). We shall not repeat them in detail, but merely state the transformations and the final form. First we write

$$U = U_0(X, Y, T) + O(Z^2), \quad V = V_0(X, Y, T) + O(Z^2), \tag{24}$$

$$W = Z\exp[1-(1+p^2)^{\frac{1}{2}}]\, W_1(X, Y, T) + O(Z^3), \tag{25}$$

and allow for negative values of X by permitting p to become negative. When $p < 0$ the sign of S in (18) must be changed, and generally $X = S\,\mathrm{sgn}\,p$ in the limit $Z \to 0$. On the lecside line of symmetry $p < 0$.

We now substitute (24) and (25) into (13) *et seq.* and take the limit $Z \to 0$. The external velocity components reduce to

$$U_{0e} = \frac{p\cos\alpha - 2\sin\alpha}{(1+p^2)^{\frac{1}{2}}}, \quad W_{1e} = \frac{[(1+p^2)^{\frac{1}{2}}+1]\cos\alpha + 2p\sin\alpha}{(1+p^2)^{\frac{1}{2}}}. \tag{26}$$

To put the equations into the most convenient form for numerical integration of the impulsive problem, with primes denoting differentiation with respect to η, we write

$$\eta = \frac{Y}{(1+p^2)^{\frac{1}{4}}T^{\frac{1}{2}}}, \quad \overline{V}_0 = T^{-\frac{1}{2}}(1+p^2)^{\frac{1}{4}}V_0 - \frac{\eta p T^{-\frac{1}{2}}}{2(1+p^2)}U_0, \tag{27}$$

$$U_0 = U_{0e}f', \quad W_1 = g', \tag{28}$$

where f and g are functions of p, η and T. Then

$$\overline{V}_0 = -U_{0e}\frac{\partial f}{\partial p} - f\left(a_1 U_{0e}\frac{\mathrm{d}U_{0e}}{\mathrm{d}p}\right) - a_2 g, \tag{29}$$

where

$$a_1 = \frac{p}{2(1+p^2)} - \frac{p}{(p^2+1)^{\frac{1}{2}}+1}, \quad a_2 = \frac{(1+p^2)^{\frac{1}{2}}}{1+(1+p^2)^{\frac{1}{2}}}, \tag{30}$$

and the appropriate boundary conditions for f and g are

$$\left.\begin{aligned} &f = f' = g = g' = 0 \quad \text{at} \quad \eta = 0, \\ &f' \to 1, \quad g' \to W_{1e} \quad \text{as} \quad \eta \to \infty. \end{aligned}\right\} \tag{31}$$

The momentum equations reduce to

$$f''' + P_1 ff'' + P_6 gf'' + P_2[1-(f')^2] + P_{13}nf'' = P_7\frac{\partial f'}{\partial T} + P_{10}\left(f'\frac{\partial f'}{\partial p} - f''\frac{\partial f}{\partial p}\right), \tag{32}$$

$$g''' + P_1 fg'' + P_6 gg'' + P_3(f')^2 + P_4(g')^2 + P_5 f'g' + P_{12} + P_{13}\eta g'' = P_7\frac{\partial g'}{\partial T} + P_{10}\left(f'\frac{\partial g'}{\partial p} - g''\frac{\partial f}{\partial p}\right), \tag{33}$$

where

$$\left.\begin{aligned} P_1 &= T\left(a_1 U_{0e}+\frac{\mathrm{d}U_{0e}}{\mathrm{d}p}\right), \quad P_2 = T\frac{\mathrm{d}U_{0e}}{\mathrm{d}p}, \quad P_3 = TU_{0e}^2, \quad P_4 = -Ta_2, \\ P_5 &= Ta_3 U_{0e}, \quad P_6 = Ta_2, \quad P_7 = T(1+p^2)^{\frac{1}{2}}, \quad P_{10} = TU_{0e}, \\ P_{12} &= T\left(U_{0e}^2+a_2 W_{1e}^2-a_3 U_{0e} W_{1e}+U_{0e}\frac{\partial W_{1e}}{\partial p}\right), \quad P_{13} = \tfrac{1}{2}(1+p^2)^{\frac{1}{2}}, \end{aligned}\right\} \tag{34}$$

$$a_3 = \frac{p}{(1+p^2)^{\frac{1}{2}}}+\frac{p}{1+(1+p^2)^{\frac{1}{2}}}.$$

These two equations (32) and (33) are in a convenient form for numerical integration, since at $T = 0$, f, g and their derivatives are given by

$$\left.\begin{aligned} f &= \eta\,\mathrm{erf}(\lambda\eta)-\frac{1}{\lambda\sqrt{\pi}}(1-\mathrm{e}^{-\lambda^2\eta^2}), \quad g = W_{1e} f, \\ f' &= \mathrm{erf}(\lambda\eta), \quad g' = W_{1e} f', \\ f'' &= \frac{2\lambda}{\pi^{\frac{1}{2}}}\mathrm{e}^{-\lambda^2\eta^2}, \quad g'' = W_{1e} f'', \end{aligned}\right\} \tag{35}$$

where $$\lambda = \tfrac{1}{2}(1+p^2)^{\frac{1}{4}}.$$

Further, the integration in the direction of increasing p may be assumed to start at the stagnation point $p = 2\tan\alpha$, where f and g are independent of p and satisfy partial differential equations in η and T only, and proceeds in a straightforward way since $U_{0e} > 0$ when $p > 2\tan\alpha$. A similar remark applies to the integration in the direction of decreasing p, since $U_{0e} < 0$ when $p < 2\tan\alpha$.

3. Solution procedure

The numerical solution of equations (32) and (33) was obtained using the Box method, a two-point finite-difference method developed by H. B. Keller and extensively used for two-dimensional flows, both steady and unsteady, and for three-dimensional steady flows. Here we use two versions of the Box method, the regular box in regions where $f' \geqslant 0$ across the layer, and the zigzag box in regions where $f' < 0$ at any value of η. Specifically, in advancing the solution to a new value of T or p, this property of f' determined the choice of the box scheme. The details of the box scheme are described in Bradshaw, Cebeci & Whitelaw (1981).

Calculations of the unsteady boundary layers were carried out for angles of attack α of 30°, 40°, 45° and 50°. Provided that flow reversal did not occur, the solution of the equations by the regular box was appropriate, no numerical difficulties were encountered and the solution was smooth. The step sizes chosen for all computations were $\Delta p = 0.2$ and $\Delta T = 0.2$; in selected cases comparisons were made with studies using step sizes of $\Delta p = 0.1$ and $\Delta T = 0.1$ or smaller, and the differences were negligible. However, once flow reversal occurred, the regular box became prone to instabilities and was replaced in this domain by the zigzag box over all η and the step sizes in p and T were reduced. Various calculations were carried out with a non-uniform mesh in p and T in the neighbourhood of separation. The smallest value of Δp was 0.0005 near the separation point; the step size in T was progressively reduced as the calculations proceeded, the smallest value being 0.01. Elsewhere Δp was fixed at 0.2. Comparisons with solutions using larger step sizes gave confidence

that the results were reliable outside the separated region for $T < 7$, but that inside the separated region smaller step sizes in p and T were necessary to avoid small oscillations which developed for $T > 5.5$ at $\alpha = 50°$.

4. Results

The principal properties of the unsteady boundary layers are the skin-friction components defined by

$$U_0'(0,p,T) = T^{-\frac{1}{2}}U_{e0}f''(0,p,T) = (1+p^2)^{\frac{1}{4}}\left(\frac{\partial U_0}{\partial Y}\right)_w, \tag{36a}$$

$$W_1'(0,p,T) = T^{-\frac{1}{2}}g''(0,p,T) = (1+p^2)^{\frac{1}{4}}\left(\frac{\partial W_1}{\partial Y}\right)_w, \tag{36b}$$

and the displacement thicknesses defined by

$$\Delta_1(p,T) = U_{0e}T^{\frac{1}{2}}\lim_{\eta\to\infty}(\eta - f) = (1+p^2)^{-\frac{1}{4}}\int_0^\infty (U_{0e}-U_0)\,\mathrm{d}Y, \tag{37a}$$

$$\Delta_2(p,T) = T^{\frac{1}{2}}\lim_{\eta\to\infty}(\eta W_{1e} - g) = (1+p^2)^{-\frac{1}{4}}\int_0^\infty (W_{1e}-W_1)\,\mathrm{d}Y. \tag{37b}$$

These are displayed in figure 2 for $\alpha = 30°$ when separation does not occur. In figure 3 we display the properties of U_0' for $\alpha = 40°$, a solution that is on the verge of separation, and in figure 4 we show all the functions (36) and (37) for $\alpha = 50°$ when separation clearly occurs. Where appropriate, the corresponding steady-state results of Cebeci *et al.* (1980) are included in these graphs for comparison purposes.

The graphs show that for $p > 0$, i.e. on the windward line of symmetry, the steady-state solution is rapidly approached as T increases, and is essentially established for $T > 1$.

For $p < 0$, i.e. on the leeward line of symmetry, the flow properties in the steady state have two interesting features. First, for any value of α, the cross-flow displacement thickness Δ_2 rapidly decreases with p and soon becomes negative, even if separation has not occurred, and in fact is exponentially large and negative when p is large and negative. The unsteady data for $\alpha = 30°$ (figure 2*d*) confirm this trend, but the limits T finite and $p \to -\infty$ for the unsteady flow and $p \to -\infty$ for the steady flow are not interchangeable. The steady-state solution for Δ_2 becomes exponentially large and negative for $p > -2$, and the approach of the unsteady solution to the steady state has the unusual feature in that for some T, say $T > 2$, the steady and unsteady solutions agree quite well up to some negative p, after which the unsteady solutions flatten out as they approach $p \to -\infty$. As T increases, the divergence of steady and unsteady solutions occur at progressively more negative Δ_2, and as $T \to \infty$ the steady and unsteady solutions agree up to $\Delta_2 \to -\infty$.

Secondly, the steady-state meridional component U_0' of the skin friction does not tend monotonically to a limit as $p \to -\infty$, but even at small values of α has a trough followed by a peak due to the overshoot in the external velocity (26). Further, at $\alpha > \alpha_c \approx 41°$, U_0' actually vanishes at $p = p_c(\alpha)$, when p_c is a point near $p = -1$ depending on the particular choice of α. The solution is singular at this point, and the calculation must end.

The unsteady solution approaches the steady state as $T \to \infty$ for $\alpha < \alpha_c$ (figures 2 and 3), but more slowly on the windward side. Some overshoot may occur, but it is small and may be an indication of a fall-off in accuracy of either the steady-state

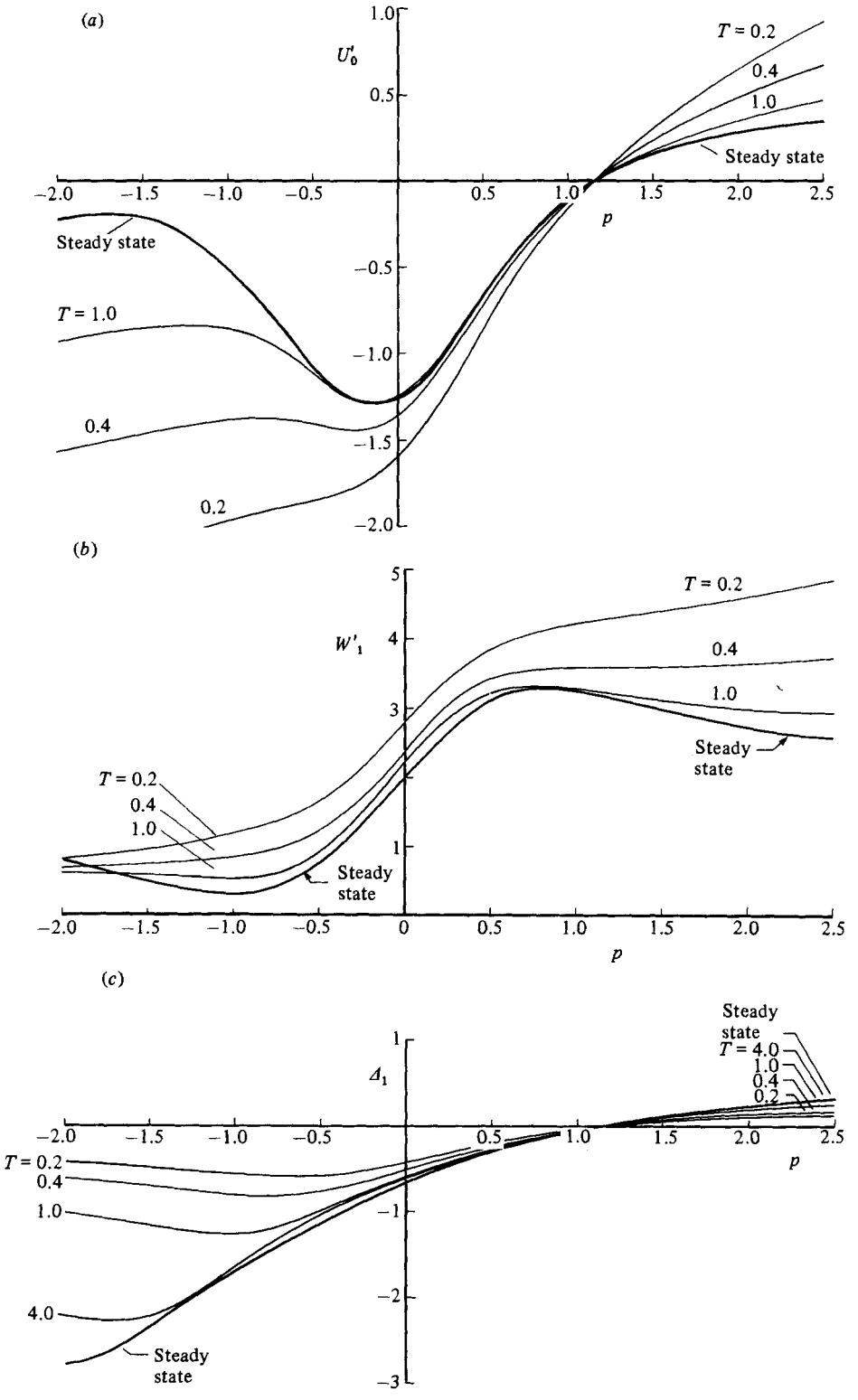

FIGURE 2 (*a–c*). For caption see p. 324.

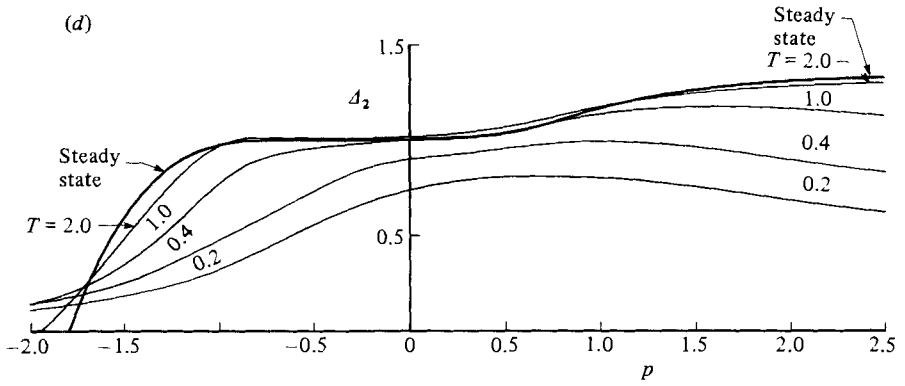

FIGURE 2. Variation of skin-friction components and displacement thicknesses with p and T for $\alpha = 30°$: (*a*) streamwise skin-friction component; (*b*) circumferential skin-friction component; (*c*) streamwise displacement thickness; (*d*) circumferential displacement thickness.

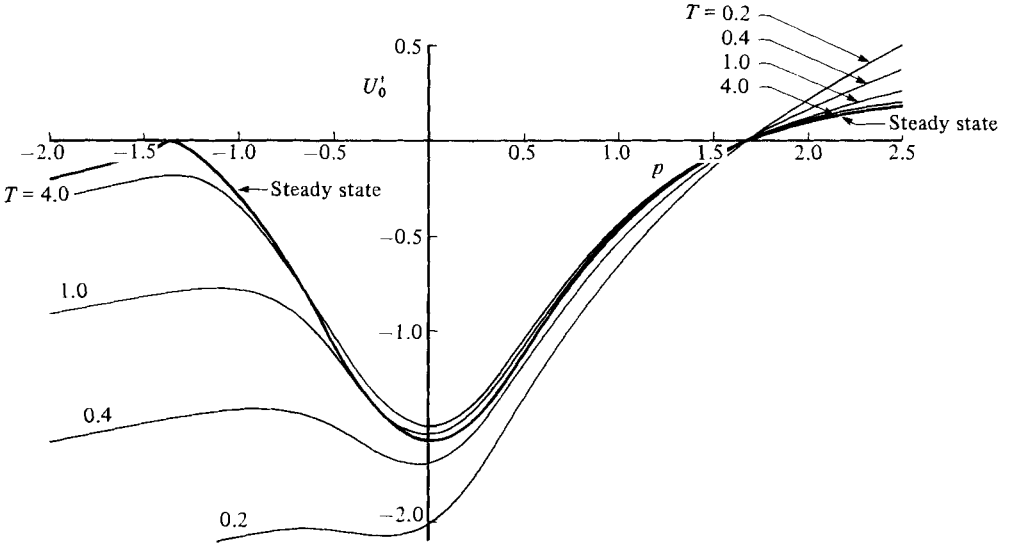

FIGURE 3. Variation of streamwise skin-friction component U_0' with p and T for $\alpha = 40°$.

or the unsteady solutions. For $\alpha > \alpha_c$ (figure 4), the same remarks apply as long as $p > p_c(\alpha)$ and flow reversal has not occurred. For smaller values of p reversed flow occurs and there is no corresponding steady-state solution. If $\alpha = 45°$ separation first occurs at $T = 5.64$ when $p = -1.2$; it remains confined within the range $-1.0 > p > -1.4$ and is weak until $T = 6$, when the computation was terminated. It might be argued that W_1' and Δ_2 are approaching limit states as $T \to \infty$, but Δ_1 is definitely showing signs of a pronounced negative minimum near $p = -1.2$.

Separation is marginal for $\alpha = 45°$, and so a more extensive computation was carried out for $\alpha = 50°$. In this case separation set in when $T \approx 3.71$ at $p = -1.083$, and gradually spread out as T increased to extend around the range $-0.908 \leqslant p \leqslant -1.396$ at $T = 6$, when the calculations became somewhat dubious owing to oscillations and instabilities, a behaviour previously observed in relation to the circular cylinder started impulsively from rest (Cebeci 1982). The behaviour of the separated solutions of U_0' for $p < -1$ and $4 \leqslant T \leqslant 6$ are shown in figure

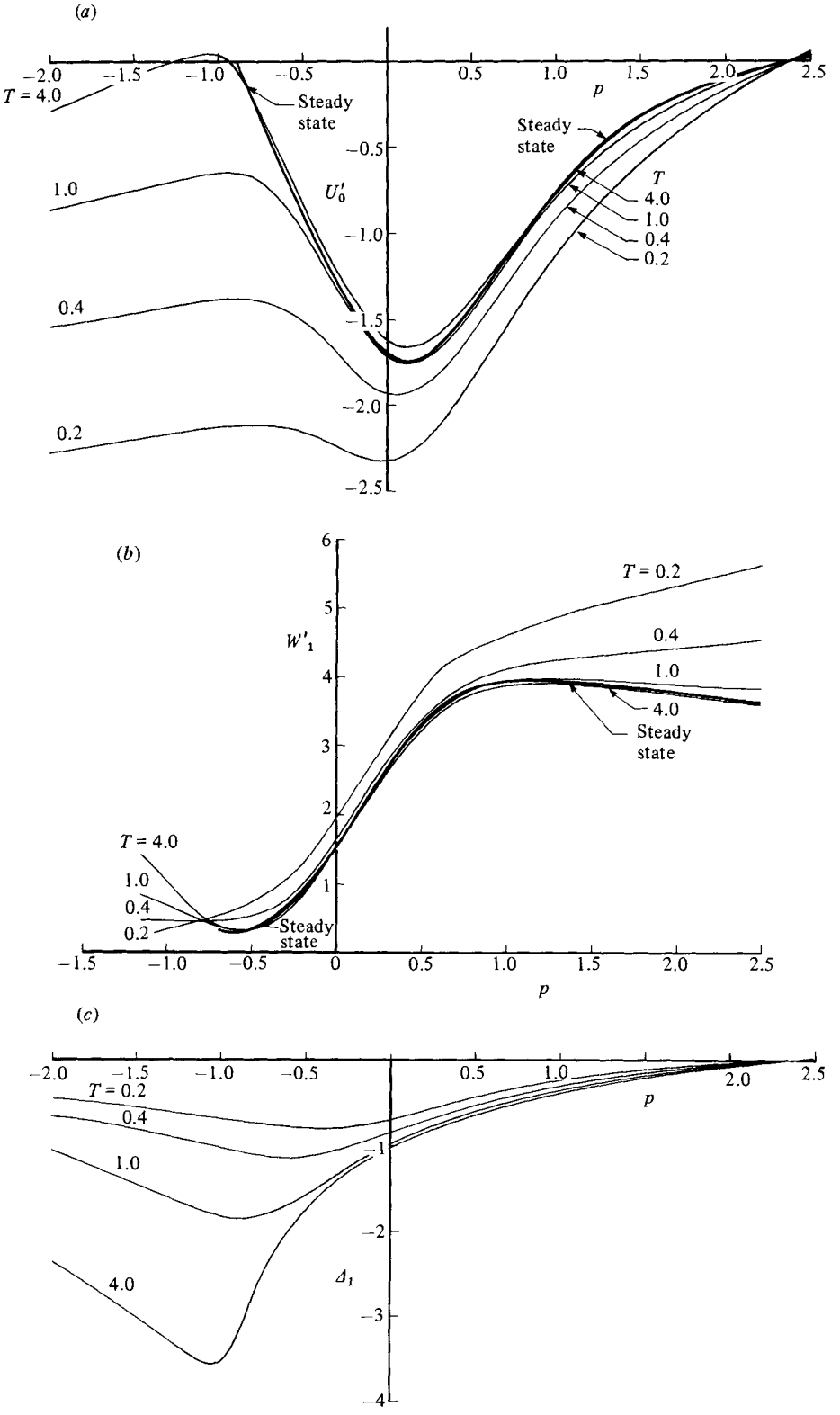

FIGURE 4(*a–c*). For caption see p. 326.

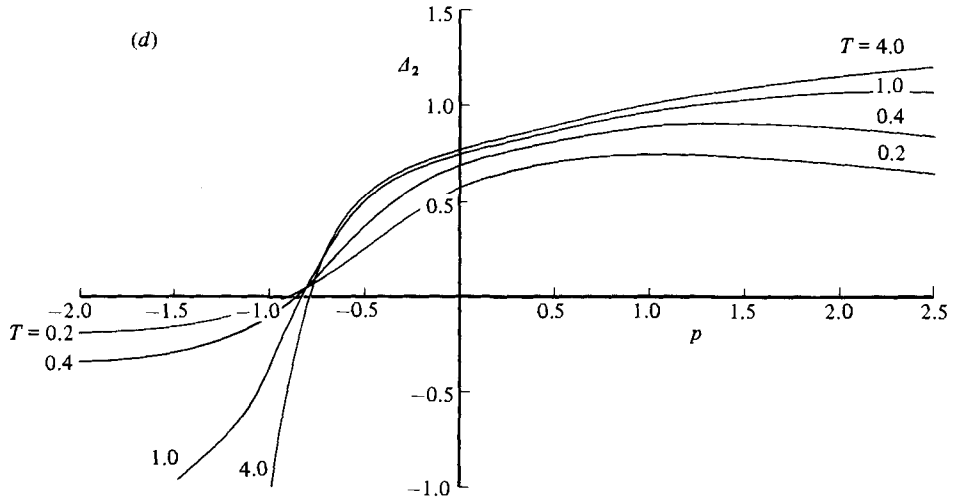

FIGURE 4. Variation of skin-friction components and displacement thicknesses with p and T for $\alpha = 50°$: (*a*) streamwise skin-friction component; (*b*) circumferential skin-friction component; (*c*) streamwise displacement thickness; (*d*) circumferential displacement thickness.

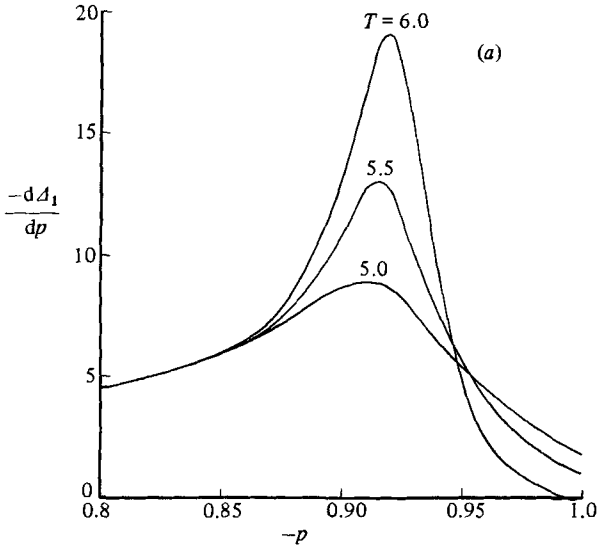

FIGURE 5(*a*). For caption see facing page.

5(*b*), indicating that reattachment occurs in this time interval. It is inferred that, after slightly larger time than $T = 6$, reattachment does not occur, and separation approaches that of steady state ($p = 0.91$), as corroborated by figure 5(*a*), where Δ_1 develops a rapid growth rate. The curves of Δ_2, not shown for $p < -1$ in figure 4(*d*), do not develop any unusual features, they become monotonically more negative as p decreases, and in addition the curves for $T > 4$ are practically coincident with the $T = 4$ curve to at least $p = -2$. Over the range of T considered ($T < 6$) the variations of Δ_2 and W_1' appear to remain smooth, but U_0' and Δ_1 develop sharp extrema just downstream of separation.

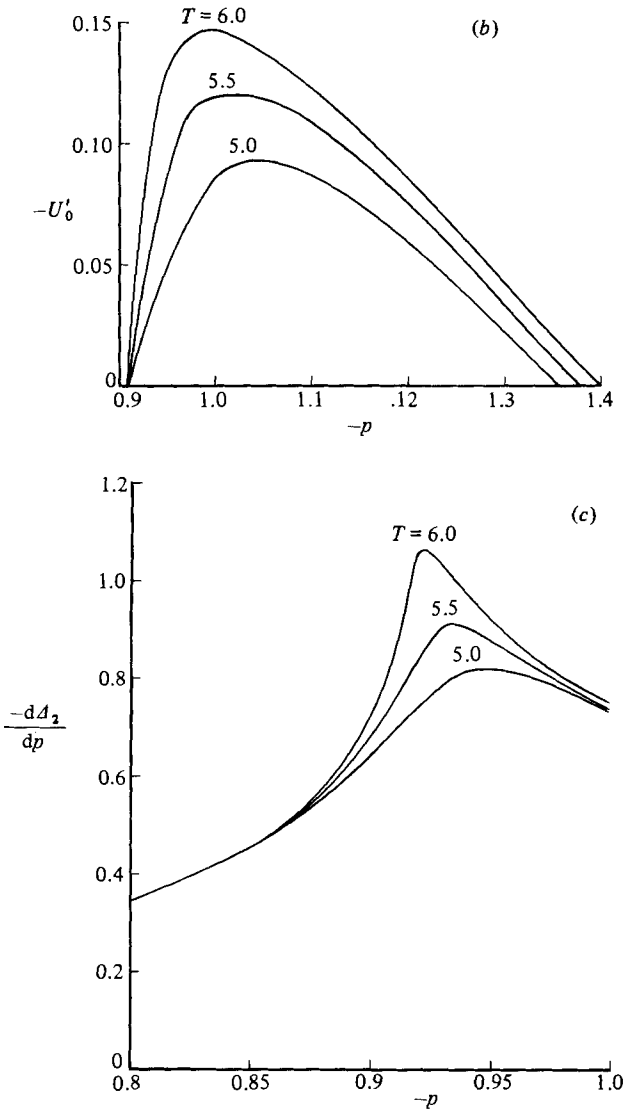

FIGURE 5. Computed results for $\alpha = 50°$: (*a*) streamwise displacement velocity; (*b*) streamwise skin-friction component; (*c*) circumferential displacement velocity.

5. The singularity?

We now investigate whether the results obtained for $\alpha = 50°$ allow us to conclude that when the computation terminated the flow properties are consistent with a singularity centred just downstream of separation in the neighbourhood of $T = 6$.

Two possible structures for a terminating singularity to the solution have been proposed, of which one is due to Smith (1982). In his model, the viscous terms are significant at breakdown, which is a generalization of the Goldstein singularity, and both skin-friction and displacement thickness are infinite. No example of such a structure has yet been found, and, although we cannot rule out its relevance in the present flow, our inclination is to prefer the second possibility, due to van Dommelen

& Shen (1982*a*), in which the skin friction remains finite while the displacement thickness becomes infinite. Strong evidence in favour of the unsteady boundary layer on a circular cylinder behaving in the same way has been provided by van Dommelen & Shen, Cowley (1983) and Ingham (1984), and on a oscillating airfoil by Cebeci *et al.* (1983).

The essence of the singularity is inviscid and independent of the pressure gradient. Thus, in the case of a two-dimensional boundary layer, with equations

$$\frac{\partial u}{\partial x}+\frac{\partial v}{\partial y}=0, \tag{38a}$$

$$\frac{\partial u}{\partial t}+u\frac{\partial u}{\partial x}+v\frac{\partial u}{\partial y}=-\frac{1}{\rho}\frac{\partial p}{\partial x}+\frac{\partial^2 u}{\partial y^2}, \tag{38b}$$

let us suppose the singularity is centred at $t=t_0$, $x=x_0$. Then in its simplest form we write

$$u=-u_0+(t_0-t)^{\frac{1}{2}}\tilde{u}(\tilde{x},\tilde{y}) \tag{39}$$

when $0<t_0-t\ll 1$, $|x-x_0|\ll 1$, where

$$\tilde{x}=\frac{(x-x_0)-u_0(t_0-t)}{(t_0-t)^{\frac{3}{2}}},\quad \tilde{y}=y(t_0-t)^{\frac{1}{4}},$$

and the determination of $\tilde{u}$ reduces to quadratures. This structure must be matched to other structures near $y=0$ and as $y\to\infty$, but the principal gross features can be inferred from (39). The displacement thickness has a peak at $\tilde{x}=0$ which becomes infinite like $(t_0-t)^{-\frac{1}{4}}$ as $t\to t_0$. On the other hand, the skin friction remains finite as $t\to t_0$ for all x. The velocity profile becomes very flat as $t\to t_0$, provided that $\tilde{x}\sim 1$, with $u=-u_0$ over a length $(t_0-t)^{-\frac{1}{4}}$ normal to the surface, the adjustment to the boundary conditions both on the surface and at infinity taking place over effectively finite ranges of values of y. Further details of the structure of the singularity, on the basis of a Lagrangian representation may be found in van Dommelen (1981) and in Elliott, Cowley & Smith (1983), on the basis of an Eulerian representation as exemplified by (38).

This theory may be adapted to our problem at least in principle. We replace u, x, y in (39) by f', p, η, and neglect the left-hand side of (32) in the neighbourhood of $p=p_0$, $t=t_0$. Then the equation for f' is the same as that for $\tilde{u}$, and we may infer that f' is as likely to develop the van Dommelen & Shen singularity as is u in the circular-cylinder problem. The displacement thickness Δ_1 can be expected to develop an increasingly sharp peak as t is increased, whereas the corresponding component of skin friction U_0' remains finite and smooth.

The evidence in figure 4 supports these conclusions, but a more severe test is to plot the streamwise displacement velocity $\partial\Delta_1/\partial p$ as a function of p for various T, and this is done in figure 5(*a*) after smoothing the data for $p<-0.95$. The results of Cowley (1983) for the solution of (38) with $u_e=\sin x$ show that the singularity occurs at $T\approx 3.0$. The similarities in form are striking; the principal difference being a slight drift in $\partial\Delta_1/\partial p$ away from separation as T increases. The more detailed plots of U_0' in figure 5(*b*) confirm the smooth behaviour of this function.

If now we examine (33) we see that the same form for g' may be assumed provided that g_0' is taken equal to f_0', and again the left-hand side of (33) may be neglected. This means that Δ_2 should also develop a needle-like singularity, and figure 4(*d*) shows no evidence of this. However, plots of $\partial\Delta_2/\partial p$ as functions of p for various T, displayed in figure 5(*c*), show clear signs of the development of a strong minimum, similar to

that of Cowley (1983), which does drift towards separation. The alternative possibility that Δ_2 is finite seems to require that, as η increases, g' has reached the value W_{1e} before the inviscid zone $\eta \approx 1$ is reached. Were this the case, the two sides of (33) would not balance over this zone, since then $f' \approx f_0' \neq 1$.

6. Discussion

In this paper we have examined the evolution of the unsteady boundary layer on the line of symmetry of a paraboloid that is set impulsively into motion at $T = 0$ with uniform velocity and at an angle of attack α. We have shown that if $\alpha < \alpha_c$ ($\approx 41°$) and the steady-state boundary layer exists everywhere on this line, the unsteady solution approaches it reasonably quickly and without any significant special features. The same is true for $\alpha > \alpha_c$ on the windward side. On the leeward side the steady-state boundary layer separates, and the solution must terminate there because the external pressure gradient is fixed. The unsteady boundary layer is initially unseparated, but develops a region of reversed flow after a finite time. A short time later the first displacement thickness Δ_1 develops a pronounced peak, and we advance arguments for believing that this is associated with an incipient singularity which terminates the calculation.

The results obtained here are also relevant to other bodies, most obviously prolate spheroids, but others as well. Our earlier studies demonstrated that in the neighbourhood of the nose the governing equations for a spheroid can be transformed into a form in which the paraboloid equations appear as a natural limit ($\tau \to 0$, see (17)) in which the various parameters of the flow remain finite. Hence we may confidently expect that any special feature, such as separation, which appears in the one will also appear in the other. Wang & Fan (1982) have studied the unsteady boundary on a prolate spheroid for $\alpha = 45°$ for a value of τ of 0.25, and found that the unsteady boundary layer did not separate for any t but that the steady-state boundary layer separated at $p = 0.39/\tau$. This result may be in conflict with ours, and moreover is a matter of surprise. For not only does a small non-zero τ make very little difference to our form of the equations, but the result is hard to understand in the general context of boundary-layer theory. At present the discrepancy is inexplicable. The choice of coordinate systems for integration around the nose does seem to be very cumbersome, and it would be interesting to repeat the calculations using the system advocated here. For the purposes of this discussion we shall set this calculation at one side.

We repeat therefore that in our view the phenomena we have discussed in connection with the paraboloid would also appear in a comparable study of prolate spheroids. In particular, the singularity would appear after a finite time in an integration of the unsteady equations on the line of symmetry in the neighbourhood of the nose and just downstream of separation if $\alpha > \alpha_c$. Generalization of this conclusion to the unsteady boundary layer over the whole spheroid is of interest. In principle the integration of four-dimensional boundary-layer equations (x, θ, y, t) wavelike with respect to (x, θ, t) using the Keller-box scheme is no more difficult than those for steady two-dimensional flow, provided that we make appropriate modifications to account for the varying direction of flow across the boundary layer. It just takes longer because there are more mesh points to consider in the (x, θ, t)-space. We may expect that the solution of these equations will develop a singularity on the normals to a curve C on the spheroid after a finite time, the precise time varying from point to point of C, and it will be inviscid in character. Indeed van Dommelen & Shen

(1982*b*) (see also Cowley 1983) have suggested a generalization of their two-dimensional structures which seems likely to be appropriate. From our experience with two-dimensional unsteady boundary layers we are confident that the Keller-box scheme can carry the integration up to the first onset of the singularity. It remains to be seen whether the calculation can be extended beyond this time and over what part of the flow field – certainly the front portion of the body can be treated, but the precise boundaries are presumably fixed by an application of the Raetz (1957) theory of influence regions.

Finally it is of interest to consider the possible impact of this study on the calculation of steady boundary layers on bodies of revolution. The extensive computations in τ on prolate spheroids showed that on the windward part of the separation line the flow field develops a Goldstein–Brown (see Brown 1965) singularity. On the leeside of the ok of accessibility (Cebeci, Khattab & Stewartson 1981*b*), the calculations for large α must, in general, be terminated by the external streamline through the ok, so that the question of the structures of the leeside separation line is irrelevant. At small values of α ($\approx 6°$) this limitation does not apply, but nevertheless the computation breaks down. It is believed that this breakdown occurs very near leeside separation, but a reconciliation with the Goldstein–Brown structure was not achieved. In particular, the blowing velocity is *negative*, whereas the theory requires it to be large positive.

A feature of the singularity is that, when $t_0 - t$ is small (39), the blowing velocity is large and positive as $x \to x_0$, and after peaking becomes negative in order to bring the displacement thickness back to more moderate values. Thus there is some parallel here with the leeside separation. Further encouragement to this notion comes from the structure (39), which suggests that, in the central regime of the singularity, the velocity components are almost constant. If this is the case, in the leeside separation singularity the governing equations for steady three-dimensional and unsteady two-dimensional boundary-layer flow are effectively the same, and so the assumption of a van Dommelen & Shen singularity is as consistent for the one class as the other.

This research was supported under Air Force Office of Scientific Research contract F49620-82-C-0055 and under the National Science Foundation Grant MEA-8018565.

REFERENCES

Bradshaw, P., Cebeci, T. & Whitelaw, J. H. 1981 *Engineering Calculation Methods for Turbulent Flows*. Academic.

Brown, S. N. 1965 Singularities associated with separating boundary layers. *Phil. Trans. R. Soc. Lond.* A **257**, 409–444.

Carr, L. W. & McAlister, K. W. 1983 The effect of a leading-edge slat on the dynamic stall of an oscillating airfoil. *AIAA Paper* 83-2533.

Carr, L. W., McAlister, K. W. & McCroskey, W. J. 1977 Analysis of the development of dynamic stall based on oscillating airfoil experiments. *NASA TN* D-8382.

Cebeci, T. 1979 The laminar boundary layer on a circular cylinder started impulsively from rest. *J. Comp. Phys.* **31**, 153–172.

Cebeci, T. 1982 Unsteady separation. In *Numerical and Physical Aspects of Aerodynamic Flows* (ed. T. Cebeci), pp. 265–277. Springer.

Cebeci, T. & Carr, L. W. 1981 Prediction of boundary-layer characrteristics of an oscillating airfoil. In *Unsteady Turbulent Shear Flows* (ed. R. Michel, J. Cousteix & R. Houdeville), pp. 145–158. Springer.

CEBECI, T. & CARR, L. W. 1983 Calculation of boundary layers near the stagnation point of an oscillating airfoil. *NASA TM* 84305.

CEBECI, T., KHATTAB, A. A. & SCHIMKE, S. M. 1983 Can the singularity be removed in time-dependent flow? In *Proc. A.F. Workshop, Colorado Springs, CO.*

CEBECI, T., KHATTAB, A. A. & STEWARTSON, K. 1980 On nose separation. *J. Fluid Mech.* **97**, 435–454.

CEBECI, T., KHATTAB, A. A. & STEWARTSON, K. 1981*b* Three-dimensional laminar boundary layers and the ok of accessibility. *J. Fluid Mech.* **107**, 57–87.

CEBECI, T., STEWARTSON, K. & WILLIAMS, P. G. 1981*a* Separation and reattachment near the leading edge of a thin airfoil at incidence. *AGARD Conf. Proc.* 291, *Paper* 20.

COUSTEIX, J., HOUDEVILLE, R. & JANELLE, J. 1981 Response of a turbulent boundary layer to a pulsation of the external flow with and without adverse pressure gradient. In *Unsteady Turbulent Shear Flows* (ed. R. Michel, J. Cousteix & R. Houdeville), pp. 120–144. Springer.

COWLEY, S. J. 1983 On unsteady three-dimensional laminar boundary-layer separation. *J. Fluid Mech.* **135**, 389–405.

DAVIS, S. S. & MALCOLM, G. N. 1979 Experiments in transonic flow. *AIAA Paper* 79-769.

ELLIOTT, J. W., COWLEY, S. J. & SMITH, F. T. 1983 Breakdown of boundary layers: (i) on moving surfaces; (ii) in semisimilar unsteady flow; (iii) in fully unsteady flow. *Geophys. Astrophys. Fluid Dyn.* **25**, 77–138.

GEISSLER, W. 1983 Theoretical and experimental dynamic stall, investigations on a rotor tip blade. In *Proc. 2nd Symp. on Numerical and Physical Aspects of Aerodyn. Flows, Long Beach, CA.*

HIRSH, R. S. & CEBECI, T. 1977 Calculation of three-dimensional boundary layers with negative cross-flow on bodies of revolution. *AIAA Paper* 77-683.

INGHAM, D. B. 1984 Unsteady separation. *J. Comp. Phys.* **53**, 90–99.

MCCROSKEY, W. J. 1982 Unsteady airfoils. *Ann. Rev. Fluid Mech.* **14**, 285–311.

MCCROSKEY, W. J., MCALISTER, K. W., CARR, L. W. & PUCCI, S. L. 1982 An experimental study of dynamic stall on advanced airfoil sections 1, 2, 3. *NASA TM* 84245.

MEHTA, U. 1977 Dynamic stall of an oscillating airfoil. *AGARD Conf. Proc.* 227, *Paper* 23.

RAETZ, G. S. 1957 A method of calculating three-dimensional boundary layers of steady compressible flows. *Northrop Corp. Rep.* NAI58-73.

SHAMROTH, S. J. 1981 A turbulent flow Navier–Stokes analysis for an airfoil oscillating in pitch. In *Unsteady Turbulent Shear Flows* (ed. R. Michel, J. Cousteix & R. Houdeville), pp. 185–196. Springer.

SMITH, F. T. 1982 On the high Reynolds number theory of laminar flows. *IMA J. Appl. Maths* **28**, 207–281.

TELIONIS, D. P. 1979 Review. Unsteady boundary layers, separated and attached. *Trans. ASME J. Fluids Engng* **101**, 29–43.

TELIONIS, D. P. & TSAHALIS, D. T. 1974 Unsteady laminar separation over cylinder started impulsively from rest. *Acta Astronautica* **1**, 1487.

TIJDEMAN, H. 1977 Investigations of the transonic flow around oscillating airfoils. *NLR TR* 77090U.

VAN DOMMELEN, L. L. 1981 Unsteady boundary layer separation. Ph.D. thesis Cornell University.

VAN DOMMELEN, L. L. & SHEN, S. F. 1982*a* The genesis of separation. In *Numerical and Physical Aspects of Aerodynamic Flows* (ed. T. Cebeci), pp. 293–311. Springer.

VAN DOMMELEN, L. L. & SHEN, S. F. 1982*b* Boundary layer separation singularities as stationary points in Lagrangian space. Submitted for publication.

WANG, K. C. 1970 Three-dimensional boundary layer near the plane of symmetry of a spheroid at incidence. *J. Fluid Mech.* **43**, 187–209.

WANG, K. C. 1976 Separation of three-dimensional flow. In *Proc. Viscous Flow Symp., Lockheed–Georgia Co., Atlanta, Georgia.*

WANG, K. C. & FAN, Z. Q. 1982 Unsteady symmetry-plane boundary layer and 3-D unsteady separation. Part I. High incidence. *San Diego State Univ. Rep.* AEOEM TR-82-01.

WILLIAMS, J. C. 1977 Incompressible boundary-layer separation. *Ann. Rev. Fluid Mech.* **9**, 113–144.

WILLIAMS, J. C. 1982 Flow development in the vicinity of the sharp trailing edge on bodies impulsively set into motion. *J. Fluid Mech.* **115**, 27–37.

WILLIAMS, J. C. & STEWARTSON, K. 1983 Flow development in the vicinity of the sharp trailing edge on bodies impulsively set into motion. Part 2. *J. Fluid Mech.* **131**, 177–194.

YOUNG, W. H. 1982 Fluid-mechanics mechanisms in the stall process of airfoils for helicopters. In *Numerical and Physical Aspects of Aerodynamic Flows* (ed. T. Cebeci), pp. 601–615. Springer.